Int. J. Nonlinear Anal. Appl. 16 (2025) 3, 285–298
ISSN: 2008-6822 (electronic)
http://dx.doi.org/10.22075/ijnaa.2024.33253.4952

Evaluating the impact of nanomaterials on soil strength parameters

Alireza Moazzami

Department of Engineering, Faculty of Civil Engineering, University of Zanjan, Zanjan, Iran

(Communicated by Sirous Moradi)

Abstract

This aim study aims at investigating the impact of nanomaterials on the soil strength parameters. This project is carried out according to the laboratory tests to determine the impact of nano-silica on the compressive strength and plasticity properties of soil. This project covers the operation of injecting nano-silica into the remolded soil of University region, and performing the CPT test as the executive studies in addition to the analysis of nanoparticles by SEM (scanning electron microscope) and AFM (atomic force microscope) images of soil samples. These tests are done for two methods of with and without nanomaterials, and then the results are compared. According to results, nano-silica increases the Plastic Limit (PL) slightly and Liquid Limit (LL) considerably; hence, the addition of nano-silica will increase the Plasticity Index (PI) of soil. Following the increase in nano-silica, the soil compressive strength is also increased; and the more the curing time is increased, the more the compressive strength will be enhanced. The average rate of increase in compressive strength with time will be increased by increasing the percentage of nano-silica. Based on the results of field and laboratory tests for injection of nano materials and according to silica cementation between soil particles, the nano-silica injection has resulted in the increased CPT strength of soil; hence it is offered as a suitable solution.

Keywords: (Nano-silica, injection, SEM and AFM analyses, strength parameters)
2020 MSC: 82D80, 97M50

1 Introduction

A deep understanding of material properties and their internal structures has always been paramount in engineering and science. Materials, as natural resources, play a fundamental role in the development of tools and in meeting human needs. With recent scientific advancements, researchers have gained a more precise comprehension of materials at the atomic and subatomic levels, enabling the design and synthesis of novel molecular structures. Among these advancements, nanotechnology has emerged as a groundbreaking field. As Jafarinejad [6] states, "Nanotechnology is not a part of the future, but it is the whole future." Nanotechnology is manipulating and controlling matter at the molecular and atomic scales to create new materials, devices, and systems with enhanced properties. One of the main goals of nanotechnology research is to develop new materials or modify existing ones to achieve superior performance. The rapid growth of nanoscience has introduced a wide range of applications across scientific and industrial domains, including geotechnical engineering and soil stabilisation [3]. In geotechnical engineering, enhancing soil properties

Email address: moazzami@znu.ac.ir (Alireza Moazzami)

Received: November 2023 *Accepted:* March 2024

through additives has long been a prominent area of research. However, despite the transformative impact of nanomaterials in other engineering disciplines, their application in geotechnics has received relatively limited attention. Nanomaterials exhibit unique characteristics that differ significantly from their bulk counterparts, especially due to their scale-dependent behaviours. These characteristics have led to a shift in how materials are understood and utilised in soil improvement strategies. The Mohr-Coulomb failure criterion, which defines shear strength through cohesion and internal friction angle, is directly affected by the presence of nanoparticles. Soils enriched with nanoparticles-except for specific types like Smectite and Halloysite, generally exhibit higher cohesion and friction angles due to enhanced bonding between the particles and the surrounding matrix. Smectite, however, tends to form an electric double layer that limits particle-to-particle contact, reducing its friction angle. Halloysite's low bulk density and weak interlayer bonding similarly affect its performance under load. Conversely, fibre-shaped nanoparticles contribute to improved shear strength due to their interlocking and adsorption capabilities, functioning similarly to synthetic fibre reinforcements.

Over the past two decades, an increasing number of studies have focused on the integration of nanomaterials into soil to enhance its mechanical behaviour. Yonekura and Miwa [14] demonstrated the effectiveness of silica nanoparticles in improving the compressive strength of grouts [14]. Noll et al. [10] explored how silica nanoparticles enhance soil resistance to flow, fixation, and permeability [10]. Further, Butrón et al. [2] employed oedometer, triaxial, and pressure tests to analyse the influence of silica nanoparticles ranging from 5 to 100 nm in size, observing a progressive increase in soil strength over time. Their results revealed a transition from elastic to elastoplastic behaviour in soils treated with nanoparticles [2].

2 Different types of research tests

To evaluate the chemical characteristics that influence the choice of soil stabiliser, ph and X-ray fluorescence (XRF) analyses were conducted on the collected soil samples. In addition to these chemical assessments, a series of geotechnical tests—including particle size distribution, Atterberg limits (plastic and liquid limits), and unconfined compressive strength tests were performed on soil samples obtained from the Zanjan University campus. These tests aimed to classify the soil and determine its fundamental physical and mechanical properties. The selected soil is a fine-grained type sourced from remoulded soil in the Zanjan University area, specifically chosen for field testing and in situ nano-silica injection experiments. The measured ph of the soil is 7.5, indicating neutral to slightly alkaline conditions. The detailed results of the XRF analysis are presented in Table 1.

Table 1: XRF analysis of soil sample

Compounds	Amount (%)
SiO2 (silicon dioxide)	50.23
Al2O3 (aluminum oxide)	14.605
L.O.l	11.9
CaO (calcium oxide)	8.76
MgO (magnesium oxide)	4.34
Fe2O3 (iron III oxide - Hematite)	4.98
K2O (potassium oxide)	2.53
Na2O (sodium oxide)	1.037
MnO (manganese oxide)	0.112
SO3 (sulfur trioxide)	1.506
Cu (copper)	
P2O5 (phosphorus oxide (V))	
TiO2 (titanium dioxide)	
total	100

2.1 Test on the effect of nano-silica on plastic properties of soil

The soil of Zanjan University region is used with gradation according to Table 2.

This section investigates the impact of nano-silica addition on clay strength using the unconfined compressive strength (UCS) test. The experimental results highlight the considerable enhancement in clay resistance due to

Table 2: Soil gradation of region

Standard sieve number (BS)	Remaining weight on the sieve (Gr)	Percentage of soil remaining on the sieve	Percentage of passing soil from each sieve
#4	0	0%	100%
#6	63	4.13%	95.87%
#12	178	11.96%	84.21%
#20	304	22.35%	63.41%
#60	287	18.86%	41.4%
#80	369	23.93%	19.29%
#160	211	11.68%	7.11%
Under sieve	91	7.09%	0%
Total	1503	100%	-

Figure 1: Soil granulation test

nano-silica incorporation, which, despite being used in low concentrations, proves to be cost-effective in construction applications. When colloidal silica solutions are diluted to approximately 5% by weight, they exhibit physical properties—such as density and viscosity—similar to water. The specific solution used in this study contains 20% by weight of silica, has a viscosity of 55 cP, a pH of 10, and an average particle size of around 7 nanometers. Colloidal silica nanoparticles are formed when monomeric silicic acid (H_4SiO_4) undergoes condensation reactions, leading to the formation of siloxane (Si–O–Si) chains. As described by Iler [5], the surface of these particles is covered with unreacted silanol (Si–OH) groups. When particles interact, inter-particle siloxane bonds are formed, as illustrated in Figure B3. As particle size increases, further growth can be halted by adjusting the pH level. Raising the pH leads to ionization of particle surfaces, inducing repulsive forces that stabilize the suspension. Gelation time—the period required for the suspension to transform into a gel—can be managed by controlling these repulsive forces. Reducing them causes particle aggregation, forming larger clusters and eventually solidifying into a gel. The rate of gelation is directly related to the speed of particle interactions. To prevent premature gelation and enhance the stability of colloidal silica solutions, alkaline substances such as sodium hydroxide are commonly used as stabilizers [5].

A repulsive force is generated between colloidal silica particles when the pH is equal to or greater than 8, due to the presence of negatively charged oxygen ($-O^-$) groups on the particle surfaces. In the pH range of 5 to 8, $-O^-$ groups on one particle can interact with hydrogen atoms on another, forming Si–O–Si bonds. At pH values of 5 or lower, particles become neutral or may exhibit slight repulsion [5]. Alkaline conditions enhance the negative surface charge of particles through reactions with hydroxide ions, increasing electrostatic repulsion among them, as illustrated in Figure 3a. While the addition of hydroxide ions promotes gelation, colloidal silica exhibits reduced reactivity at very high pH levels due to excessive surface charge. As the pH decreases, the concentration of hydroxyl ions also declines, which in turn reduces the surface charge of the particles. Under these conditions, particles are more likely to interact and form siloxane (Si–O–Si) chains, as depicted in Figure 3b. According to Iler [5], the shortest gelation time occurs at a pH between 5 and 6. When the pH falls below 5, hydroxyl ions are removed, and particle surfaces become uncharged (Figure 3c), slowing the formation of siloxane chains and thus prolonging the gelation time. In practical terms, colloidal silica solutions with a viscosity of less than 100 cP can effectively penetrate loose sands when injected using low-head pressures and extraction wells. As the viscosity increases, a solid gel forms. The “gelation time” refers to the interval between the end of the mixing process and the initial formation of the gel. The subsequent duration—between gel formation and strength testing—is known as the “curing time.” Colloidal silica is expected to

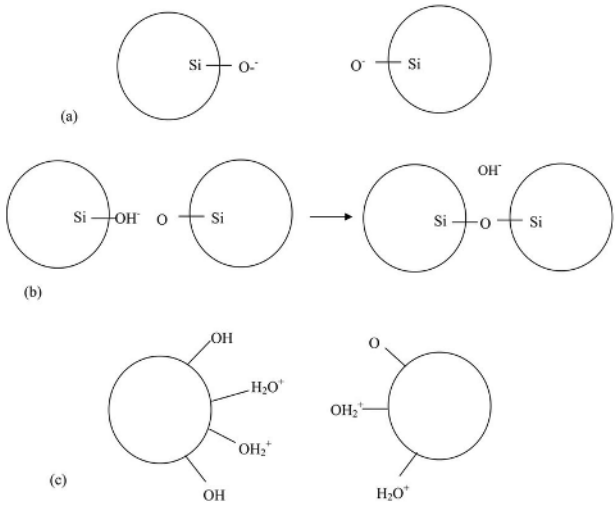

Figure 2: Behavior of colloidal silica particles in various rates of pH [16]

remain stable below the ground surface over long periods. Whang [13] estimated its lifespan to exceed 25 years, in contrast to sodium silicate and acrylate grouts, which typically have life expectancies ranging from 10 to 20 years.

2.2 Soil injection test

From an engineering perspective, **problematic soils** refer to those types of soils that are unsuitable for safe structural construction and are significantly influenced by environmental and weather conditions. These soils encompass various categories such as expansive soils, highly water-absorbent soils, collapsible soils, and loose soils. However, this study specifically focuses on **remolded soils**.

The presence of remolded soils poses a major geotechnical issue in many areas of Zanjan, where it has led to noticeable **building subsidence** across several neighborhoods. In response to this concern, a comprehensive field survey was initiated to identify appropriate test sites. This process culminated in the selection of **five separate regions**, and the proposed locations were officially submitted in a letter to the **Department of Construction at Zanjan University** to obtain the necessary permits. Following this request, the Department approved a site with remolded soils for the field tests. Initially, the study was to focus on **liquefiable soils**, but due to their limited occurrence in Zanjan, the research focus was redirected to **remolded soils**, which represent a more widespread and pressing problem across the city, contributing to significant ground settlement and structural damage.

To address this issue, selected **nanomaterials** are to be injected into the problematic soils to enhance their strength and stability. From an operational perspective, **soil injection methods** are generally classified into two categories:

- **Experimental**
- **Executive**

2.2.1 Experimental injection

The **experimental injection** phase serves as the initial stage of the injection process, conducted prior to the main **executive injection**. This stage is crucial for collecting essential data and fine-tuning the parameters required for successful large-scale application. During this phase, various slurry mixtures were formulated and injected into the soil at different concentrations to assess their infiltration characteristics and overall performance. A key objective of the experimental phase was to evaluate the **infiltration capacity** of the injected materials in remolded soil. The findings revealed that **gravity-driven injection** was ineffective due to the soil's inherently low permeability. As a result, it became necessary to adopt a **pressure injection method**. To test this approach, an injection hole was drilled into the test container, and the material was injected using a pressure pump operating at **3 bars** (equivalent to approximately 3 atmospheres). The results confirmed that this pressure was both adequate and efficient for delivering the stabilizing agents into the selected soil matrix.

2.3 Cone Penetration Test (CPT)

The **Cone Penetration Test (CPT)** was conducted by *Mahan Zamin Consulting Engineering Company* using equipment compliant with **German standards**, as illustrated in the figure below. The test results, derived from measurements taken at **30 cm depth**, were analyzed and corrected based on the specifications shown in **Sketch (5-7)**. The CPT findings demonstrate a **more than twofold increase in soil strength** following the injection of **nano-materials**. Additionally, the **duration of curing time** was found to play a significant role in the strength development process, indicating that both the presence of nano-materials and the time elapsed after injection are critical factors in enhancing soil performance.

3 Research results

3.1 Results of studies impact of nano-silica on the compressive strength of soil

Silica nanoparticles, with an average particle size of **15 nm**, were utilized in powdered form as illustrated in **Figure 1**. To prepare the test samples, **nano-silica was added to soil** (passing through a **No. 40 mesh sieve**) in weight percentages of **0.5%, 1%, 1.5%, 2%, and 3%**. The mixing process continued for approximately **45 minutes** to ensure the uniform distribution of nanoparticles and achieve **homogeneous samples**.

Subsequently, **Atterberg limit tests**—specifically, the **plastic limit** and **liquid limit**—were performed in accordance with **ASTM D4318**. The **plastic limit** was determined using the **3 mm thread rolling method**, while the **liquid limit** was measured with **Casagrande's apparatus**.

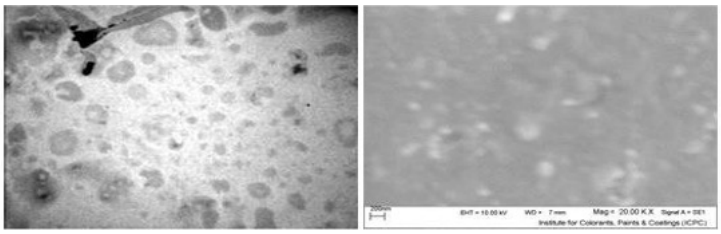

Figure 3: SEM image of nanoparticles (left), and TEM image of nanoparticles (right)

SEM and **TEM** images reveal the **silica nanoparticles** and their respective dimensions, with **TEM** offering superior image quality compared to **SEM**. The results indicate that the addition of **nano-silica** results in a slight increase in the **plastic limit (PL)**, while significantly enhancing the **liquid limit (LL)**. As a result, the incorporation of **nano-silica** leads to a notable increase in the **Plasticity Index (PI)**.

Table 3: Atterberg smoke of soil by addition of nano-silica

Nano-silica percentage	PL (%)	LL (%)	PI (%)
0	18.56	33.2	12.5
0.5	19.21	35.11	15.46
1	19.73	36.78	17.93
1.5	20.38	39.1	19.5
2	21	40.05	20.89
3	22.13	41.42	21.2

Therefore, nano-silica can be a perfect candidate to improve the soils which need higher plastic properties. The clay core of earth dams is among these cases when the access to appropriate credit sources needs consumption of much time and cost.

3.2 Results of consumed nano-silica in compressive strength of soil

According to the results of uniaxial compressive strength under a variety of curing time with different percentages of nano-silica in Table 4 and based on the provided diagrams, the compressive strength of samples has been be significantly increased until an increase of 3% in nano-silica after 28 days. This increase is caused by reactions between nano-silica and clay and the particles' binding and silica gel setting.

Figure 4: Performing a flow limit and plastic limit test

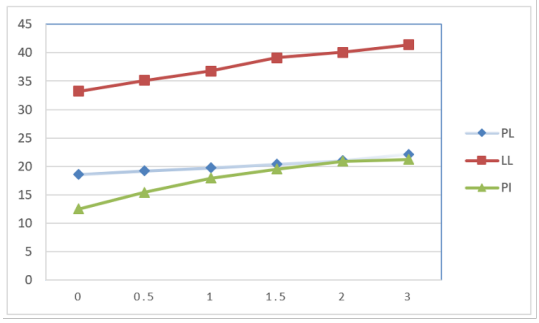

Figure 5: Changes in Atterberg's limit of soil by addition of nano-silica

Table 4: Results of compressive strength test (kg/cm2)

Sample	Strength in 7 days	Strength in 14 days	Strength in 28 days
C0	5.6	6.1	6.4
Cn0/5	8.4	14.3	20.5
Cn1	11.2	17.9	23.71
Cn1/5	11.8	33	37.8
Cn2	12.9	34.6	40.11
Cn3	15.3	27.4	46.78

In Table 4, **C0** represents the typical sample with zero percent **nano-silica**, while the **Cn0/5**, **Cn1**, **Cn1/5**, **Cn2**, and **Cn3** samples contain **0.5%**, **1%**, **1.5%**, **2%**, and **3% nano-silica**, respectively. For the **C0** sample, it is expected that there would be no significant difference in strength at **7-day**, **14-day**, and **28-day** intervals. However, **Table 4** shows a slight variation in these values, which can be explained by the following factors:
*A small percentage of organic matter in the soil may cause changes in the strength over time.
*The test error test and not-calibrated device.

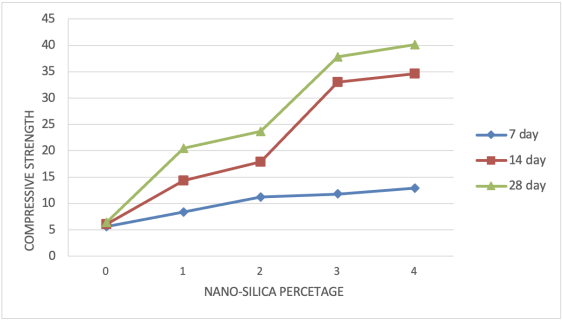

Figure 6: Diagram of changes in compressive strength by increasing the nanoparticles

Figure 7 shows the changes in peak compressive strength of **HPC** specimens after soaking for predetermined durations. In the unmodified **HPC** specimens, the compressive strength gradually decreased after soaking for 100 and 200 days, followed by a rapid decline after 300 days. The addition of **NS** helped mitigate the reduction in compressive strength, especially after 300 days, though the effect was dependent on both the concentration and soaking duration. The compressive strength of **1% NS HPC** specimens consistently exceeded that of the unmodified **HPC** specimens, increasing by **8.8%**, **17.6%**, **21.5%**, and **31.7%** after soaking for **0 days**, **100 days**, **200 days**, and **300 days**, respectively. While the compressive strengths of **2–5% NS HPC** specimens were generally higher than those of the unmodified specimens at all time points, they were consistently lower than that of the **1% NS HPC** specimens. After soaking for **200 days**, the compressive strengths of the **2–5% NS HPC** specimens were even lower than that of the unmodified **HPC** specimens.

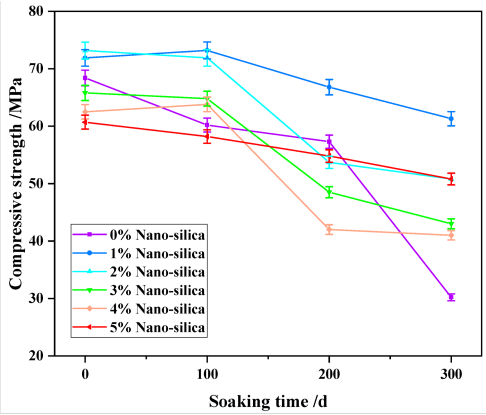

Figure 7: The time-dependent compressive strength of HPC specimens subject to sulfate attack.

3.3 Study on the microscopic structure of improved soil by nano-materials

The natural soil structure has been studied extensively by various researchers [4, 8, 9]. However, the formation of natural soil structure is often attributed to the deposition of solutions interacting with internal particles, the absence of electric charge, and Van der Waals forces, making it less applicable in comparison to hydration and pozzolanic reactions. Therefore, soil improvement is often achieved through the addition of additives.

At the nanoscale, tools and equipment play a crucial role, as working with nanotechnology would be impossible without the proper instruments. In the past, many researchers were unaware that their work was related to nanotechnology due to the lack of appropriate technology and measurement tools. As mentioned, the base elements have unique characteristics that require precise tools for their determination. In this context, applied analyses include microscopic analysis, structural analysis, elemental analysis, bonding analysis, and surface characterization, among others. Microscopic analysis has received particular attention, with SEM and AFM being used to study fine soil particles.

3.4 Analysis of scanning electron microscope (SEM)

To prepare a sample for SEM imaging, the first step is to remove water from the sample, as water would vaporize under vacuum conditions. Metals, being conductive, do not require special preparation for SEM imaging. However, non-metallic materials need to be coated with a thin conductive layer to facilitate imaging. This process is done using a tool called a sputter coater, which uses an electric field and argon gas. The sample is placed in a vacuum chamber, where electrons are separated from the argon gas due to the presence of both argon and the magnetic field. As a result, the atoms on the sample gain positive charges. The argon ions are attracted to and absorbed by a gold foil, which has a negative charge. These argon ions then collide with gold atoms on the surface of the foil, causing gold atoms to deposit onto the sample's surface, creating a conductive gold coating.

3.4.1 SEM images of soil samples

The following images are prepared from soil samples of studied region by SEM machine of Razi Research Institute.

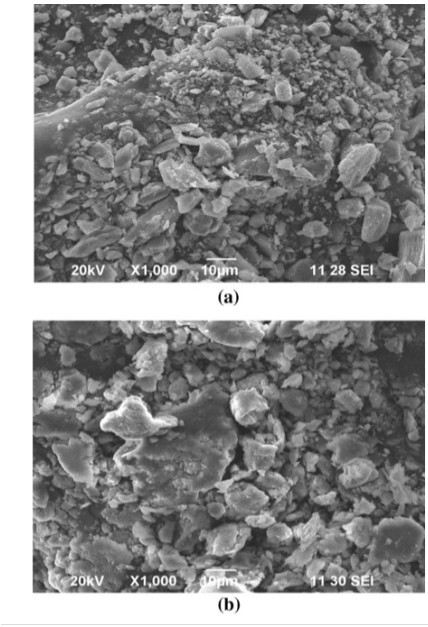

Figure 8: a SEM image of untreated clay soil. b SEM image of clay soil treated with nano-silica (7-day curing)

3.4.2 Soil analysis by atomic force microscope (AFM)

The sub-nanometer resolution of atomic force microscopy (AFM) has opened a new avenue for studying the morphology of particles. This capability has been recently demonstrated by researchers in their investigations of mineral particles [7, 11, 1]. The AFM analysis is conducted using a tool from Mahar Fan Abzar Company. AFM images of samples with added nano-silica are presented in Figures 9 to 13. These AFM images are analyzed using SPM software.

Figure 9: AFM image of a typical soil sample without nano-silica

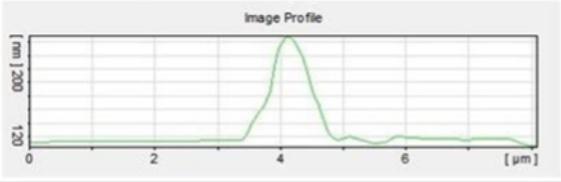

Figure 10: AFM image of soil samples with 0.5% of nano-silica

3.4.3 Surface parameters obtained from SPM Software

S_a is the average roughness which is calculated according to the following equation:

$$S_a = \int \int_{\alpha} |z(x, y)| dxdy.$$

Figure 11: AFM image of soil samples with 1% of nano-silica

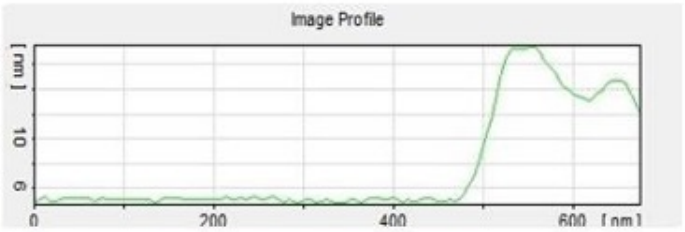

Figure 12: AFM image of soil samples with 2% of nano-silica

Figure 13: AFM image of soil samples with 3% of nano-silica

Table 5: Parameters obtained from software

Parameter	**0%**	**0.5%**	**1%**	**2%**	**3%**
S_y	19.1 nm	397 nm	51.3 nm	21.5 nm	40.12 nm
S_z	9.79 nm	305 nm	45.6 nm	23.2 nm	32.3 nm
S_a	387 pm	20.1 nm	4.98 nm	2.21 nm	7.45 nm
S_{sk}	8.93	3.85	2.56	2.87	-0.35
R_{ku}	242	20.32	9.43	11.1	3.61
S_{dq}	0.041	0.34	0.32	0.24	0.42
S_{sc}	198 mm^{-1}	1.21 μm^{-1}	3.21 μm^{-1}	22.92 μm^{-1}	127 μm^{-1}
S_{dr}	0.007%	2.01%	0.86%	2.46%	11.98%
S_{ds}	4.81 μm^{-2}	2.56 μm^{-2}	39.7 μm^{-2}	421 μm^{-2}	304 μm^{-2}
S_{td}	0	0	0	0	0
S_{ci}	0.031	0.067	0.011	0.012	0.023
S_{vi}	8.44	2.41	2.23	1.67	0.44
S_m	5.49 pm	235 pm	12.32 pm	6.45 pm	4.23 pm
S_c	16.3 nm	2.06 nm	58.3 nm	19.37 pm	5.00 pm
S_v	5.11 nm	86.55 nm	16.9 nm	5.11 nm	2.24 nm

S_{ds} is the density of summits [12]:

$$S_{ds} = \frac{\text{Number of summits} - \text{intersection number of summits}}{\text{Area}}$$

According to the results, samples with 0% and 0.5% have the minimum number of summits. This result can be seen according to the AFM image.

3.4.4 S_{sk} (Skewness of assessed profile)

Asymmetric distribution function of range measures the ADF around the reference line. The distribution function of range is the density function of sample probability for $Z(x)$ during evaluation [12].

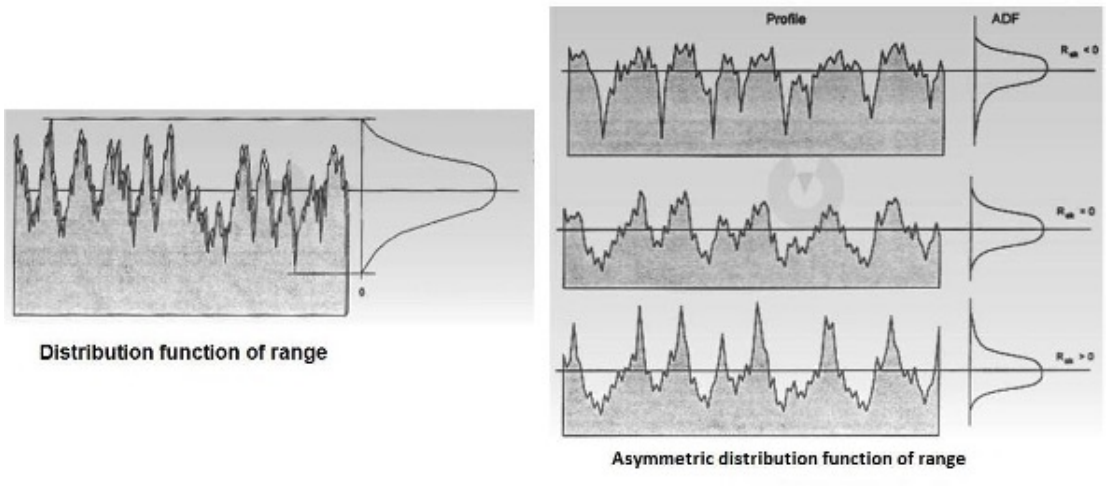

Figure 14: symmetry and asymmetry of distribution function of range [12]

A porous surface has a high $S_{sk} \cdot S_{sk} < 0$ is suitable for wear applications.

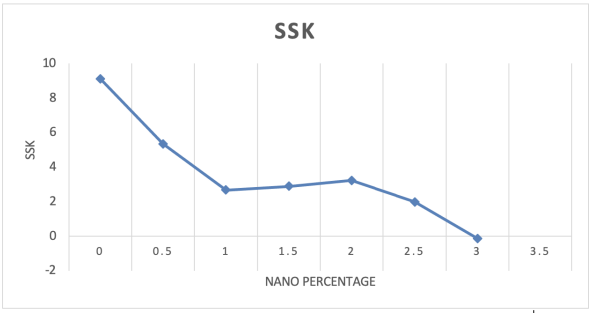

Figure 15: S_{sk} diagram in terms of nano-silica increase percentage

According to the diagram, the porosity is reduced by increasing the nono-particles. R_{ku} (kurtosis of evaluated profile [12]:

$$R_{ku} = \frac{1}{s_q^4} \int \int_{\alpha} z(x,y)^4 dxdy.$$

This amount is smaller than 3 in a sample with 3% of nano-silica. This parameter is much larger than other samples in a typical sample, and it indicates the numerous surface holes. S_{td} measures the angle between the stratification line and the y-axis [12].

3.4.5 Stratification line: Basic line and direction of surface model

S_{sc} is the total curvature of every point of surface in two perpendicular directions. Sdq is the gradient of root mean square in evaluated profile. Surface profile gradient: It is an angle of parallel line to profile with parallel line to reference line. Average gradient: Average gradient of all profile points during sampling [12].

It is applied to distinguish between the surfaces with the same Sa. Sdr is the growth rate of cleavages on the surface and it is 0% for a perfectly smooth surface [12].

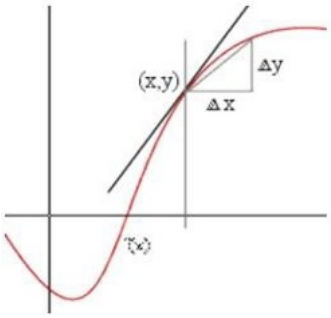

Figure 16: Average gradient

3.4.6 Matter ratio diagram

This curve shows the material ratio of profile as a function of surface height [12]. S_c is the profile height regardless of summits and deep valleys (core roughness profile).

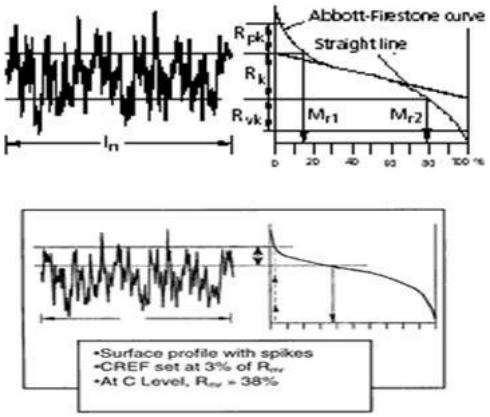

Figure 17: (S_c)

S_m: Average height of summits above the core roughness profile

The average depth of valleys below the core roughness profile (S_v), Sci and Svi are defined as follows:

$$S_{ci} = S_c/S_q$$

and

$$S_{vi} = S_v/S_q.$$

The high S_{ci} and S_{vi} indicate that the holder is good for liquid [12]. According to table data, the typical sample has higher absorption than the sample with nano-silica percentage; therefore, nano-silica reduces the water absorption. The following graph shows the changes in these parameters according to nano-silica percentage.

4 Summary and conclusion

Impact of Nano-Silica on Soil Durability

In addition to the improvements in compressive strength and plasticity, nano-silica can have significant effects on the durability of the treated soils. Specifically, the addition of nano-silica might enhance the resistance of the soil to environmental factors such as moisture, freeze-thaw cycles, and sulfate attack. This can be tested by subjecting nano-silica-modified soil samples to accelerated weathering tests or immersion in various chemical solutions. By including

core void volume
peak material volume
valley void volume

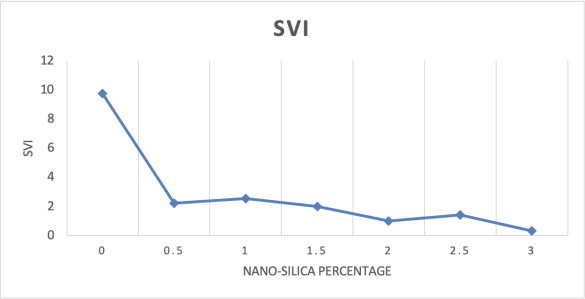

Figure 18: Changes in svi by increasing the percentage of nano-silica

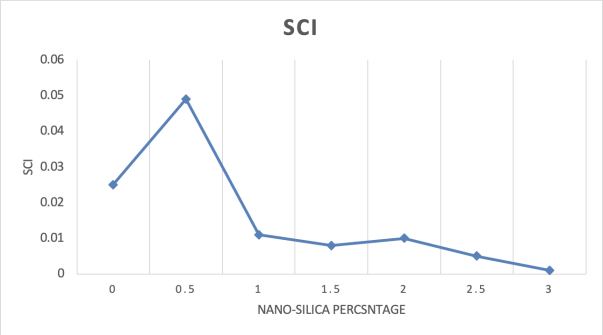

Figure 19: Changes in Sci by increasing the percentage of nano-silica

these tests, the long-term benefits of nano-silica in soil stabilization could be further validated, showcasing its role not only in strengthening the soil but also in ensuring its stability and resilience in challenging environmental conditions.

Influence of Nano-Silica on Soil Permeability

Another essential aspect to explore is how nano-silica influences the permeability of soil. As nano-silica particles are extremely fine, they may fill the voids between soil particles, thereby reducing the permeability of the soil. This property is particularly beneficial for applications where water retention or impermeability is crucial, such as in the construction of earth dams or foundations. Permeability tests, such as constant head or falling head permeability tests, could be included to measure the reduction in permeability with varying percentages of nano-silica.

Performance of Nano-Silica in Different Soil Types

Further investigation can be conducted into the effectiveness of nano-silica on different soil types. While the current study focuses on a specific soil type, including comparisons with sandy, silty, or clayey soils could help generalize the findings. Different soil types might show varied responses to nano-silica treatment, and a broader understanding of its applications could be beneficial for its practical use in different geotechnical contexts.

Effects of Nano-Silica on Soil Shrinkage and Swelling

For expansive soils, which are prone to significant volume changes due to moisture fluctuations, the addition of nano-silica could help mitigate shrinkage and swelling behaviors. A potential area for further research is the reduction in the coefficient of linear extensibility (CLE) and the soil's shrinkage index when nano-silica is applied. This can be tested by subjecting treated soil samples to swelling tests and monitoring the changes in volume.

Mechanism of Nano-Silica Action in Soil Improvement

The mechanism through which nano-silica improves soil properties could be discussed further. Detailed explanations of the chemical reactions, such as pozzolanic and cementitious reactions, can help clarify why nano-silica enhances the soil's structural integrity. The formation of silica gel during the reaction between nano-silica and soil particles can be explained in more depth, possibly with a comparison to other additives like lime or cement that are commonly used for soil stabilization.

Cost-effectiveness and Practical Application of Nano-Silica

A final consideration is the cost-effectiveness of nano-silica as a soil stabilizer. While nano-silica shows promising results in laboratory tests, its economic feasibility for large-scale construction projects should be assessed. A cost-benefit analysis comparing the price of nano-silica and its benefits in improving soil strength, durability, and plasticity should be provided. This will help decision-makers determine whether nano-silica can be a practical solution for large-scale soil stabilization applications. These additional sections will not only deepen the discussion of nano-silica's impact on soil properties but also provide a more comprehensive view of its potential applications and limitations.

In short, it can be said:

1. Nano-silica slightly increases the plastic limit (PL) but significantly increases the liquid limit (LL). Therefore, the addition of nano-silica will increase the Plasticity Index (PI) of the soil.
2. The compressive strength of soil is enhanced by increasing the percentage of nano-silica.
3. The longer the curing time, the greater the enhancement in compressive strength. The rate of increase in compressive strength over time is higher with larger percentages of nano-silica.
4. According to theoretical studies, using solid particles as a liquid solution is successful for injection at the nano-scale.
5. Based on both field and experimental tests, injecting nano-silica increases the soil's load-bearing capacity due to silica cementation between soil particles, making it a promising strategy.
6. The scanning electron microscope (SEM) is an effective method for investigating the appearance of soil, although preparing the sample for this device is challenging.
7. The atomic force microscope (AFM) provides precise geometric morphology and surface property analysis.
8. Increasing the nanoparticle concentration leads to a decrease in the surface porosity of soil particles.
9. Nano-silica reduces water absorption, and this phenomenon is observable in AFM images.

In this study, the effects of adding nano-silica to soil on its physical and mechanical properties, including Atterberg limits (PL and LL) and unconfined compressive strength (UCS), were investigated. The results showed that the addition of nano-silica to the soil led to significant changes in the soil's physical properties, including an increase in Atterberg limits (PL and LL) and improvement in unconfined compressive strength (UCS). Specifically, with an increase in nano-silica content up to 3%, the compressive strength of the soil significantly increased. These improvements were attributed to chemical reactions between nano-silica and soil particles, resulting in the formation of silica gel, which enhanced particle bonding.

Additionally, SEM and AFM microscopic analysis results indicated that the addition of nano-silica improved the microscopic structure of the soil, with soil particles becoming more effectively bonded, leading to a stronger soil structure. These findings suggest that nano-silica can be an effective material for improving soil properties, especially in applications where higher strength and stability are required.

References

[1] B.R. Bickmore, K.L. Nagy, P.E. Sandlin, and T.S. Crater, *Quantifying surface areas of clays by atomic force microscopy*, Amer. Mineral. **87** (2002), 780–783.

[2] C. Butrón, M. Axelsson, and G. Gustafson, *Silica sol for rock grouting: Laboratory testing of strength, fracture behavior and hydraulic conductivity*, Tunnel. Underground Space Technol. **24** (2009), no. 6, 603–607.

[3] A. Dowling, *Nano-science and nonotechnologies*, Int. Symp. Nature, Purposes, Ethics and Politics of Evidence in a Democracy, Vol. 61, 2006.

[4] G.W. Gee and J.W. Bauder, *Particle Size Analysis, Methods of Soil Analysis: Part I*, 2nd ed., American Society of Agronomy (Agronomy9), Madison, 1986.

[5] R.K. Iler, *The Chemistry of Silica: Solubility, Polymerization, Colloid, and Surface Properties, and Biochemistry*, Wiley, New York, 1979.

[6] Sh. Jafarinejad, *Basic Elements in Nanotechnology and Polymer Nanocomposites*, Simaye Danesh, 2009. [In Persian]

[7] M.C. Jodin, F. Gaboriaud, and B. Humbert, *Repercussions of size heterogeneity on the measurement of specific surface areas of colloidal minerals: combination of macroscopic and microscopic analyses*, Amer. Mineral. **89** (2004), 1456–1463.

[8] P.A. Johnsson, C.M. Eggleston, and M.F. Hocella, *Imaging molecularscale structure and microtopography of hematite with the atomic force microscope*, Amer. Mineral. **76** (1991), 1442–1445.

[9] K. Namjesnik-Dejanovic and P.A. Maurice, *Atomic force microscopy of soil stream fulvic acid*, Colloids Surfaces A: Physicochem. Engin. Asp. **120** (1997), 77–86.

[10] M.R. Noll and C. Bartlett, *Dochat TM in situ permeability reduction and chemical fixation using colloidal silica*, Nat. Outdoor Action Conf., Las Vegas, NV, 1992, pp. 443–57.

[11] M. Sayed Hassan, F. Villieras, F. Gaboriaud, and A. Razafitianamaharavo, *AFM and low-pressure argon adsorption analysis of geometrical properties of phyllosilicates*, J. Coll. Interf. Sci. **296** (2006), no. 2, 614–623.

[12] K. Stout, J. Sullivan, W. P. Dong, E. Mainsah, N. Luo, T. Mathia, and H. Zahouani, *The development of methods for the characterization of roughness on three dimensions*, Publication no. EUR 15178 EN of the Commission of the European Communities, Luxembourg, 1994.

[13] J.M. Whang, *Section 9: Chemical-based barrier materials*, Assessment of barrier containment technologies for environmental remediation applications, R. R. Rumer and J. K. Mitchell, eds., NTIS, Springfield, 1995, pp. 211–247.

[14] R. Yonekura and M. Miwa, *Fundamental Properties of Sodium Silicate Based Grout*, Geotech. Conf., Singapore, 1993, pp. 439–444.

[15] G. Zhang, *Advances in Measurement and Modeling of Soil Behavior*, ASCE, 2007.

[16] G. Zhang, J.T. Germaine, A.J. Whittle, and C.C. Ladd, *Index properties of a highly weathered old alluvium*, Geotechnique **54** (2004b), no. 7, 441–451.